

CORRESPONDENCE

Reply to “Comments on ‘Corrections for Pumped SBE 41CP CTDs Determined from Stratified Tank Experiments’”

KIM I. MARTINI AND DAVID J. MURPHY

Sea-Bird Scientific, Bellevue, Washington

RAYMOND W. SCHMITT

Woods Hole Oceanographic Institution, Woods Hole, Massachusetts

NORDEEN G. LARSON

Sea-Bird Scientific, Bellevue, Washington

(Manuscript received 7 October 2019, in final form 19 December 2019)


1. Introduction

The response in [Johnson \(2020\)](#) that the method used to determine cell thermal mass correction coefficients for SBE 41CP CTD data from Argo floats is biased as determined by [Martini et al. \(2019\)](#) is valid. However, the recommendation for correction coefficients should not be followed due to these three errors in [Johnson \(2020\)](#):

- 1) Alignment is as large a source of dynamic error as cell thermal mass in the SBE 41CP CTD.
- 2) Order of operations was overlooked, so that cell thermal mass is used to correct for alignment errors caused by the temporal mismatch of temperature and conductivity.
- 3) The cell thermal mass corrections determined in [Johnson et al. \(2007\)](#) and [Johnson \(2020\)](#) also bias salinity.

In this response we will do the following:

- 1) Detail how the corrections in [Johnson \(2020\)](#) are biased because the optimization procedure does not accurately model physics in the tank and conductivity cell.

 Denotes content that is immediately available upon publication as open access.

Corresponding author: Kim I. Martini, kmartini@seabird.com

- 2) Verify using in situ data from Argo floats deployed in the ocean that alignment is a significant source of error for the SBE 41CP as shown in [Martini et al. \(2019\)](#).
- 3) Determine cell thermal mass correction coefficients from the stratified tank experiment merging the methods of [Johnson \(2020\)](#) and [Martini et al. \(2019\)](#) to optimize against a model that better represents the physics in the tank and conductivity cell.
- 4) Compare the corrections using in situ data using the coefficients determined in [Johnson et al. \(2007\)](#), [Martini et al. \(2019\)](#), [Johnson \(2020\)](#), and this manuscript.

2. Bias in stratified tank analysis

[Johnson \(2020\)](#) incorrectly asserts that [Martini et al. \(2019\)](#) assumes the “temperature gradient is Gaussian but the salinity gradient is not.” Neither the temperature or salinity gradients are well defined by a Gaussian because the interface is also affected by salt fingering and microstructure ([Schmitt et al. 2005](#); [Martini et al. 2019](#)). This is why alternate methods such as symmetry and modeling the structure in the lower layer are chosen in [Martini et al. \(2019\)](#) rather than optimizing to a shape that does not completely model the gradient in the tank.

In [Johnson \(2020\)](#), the optimization procedure used to determine the cell thermal mass correction set the width and center of the salinity gradient to be unconstrained.

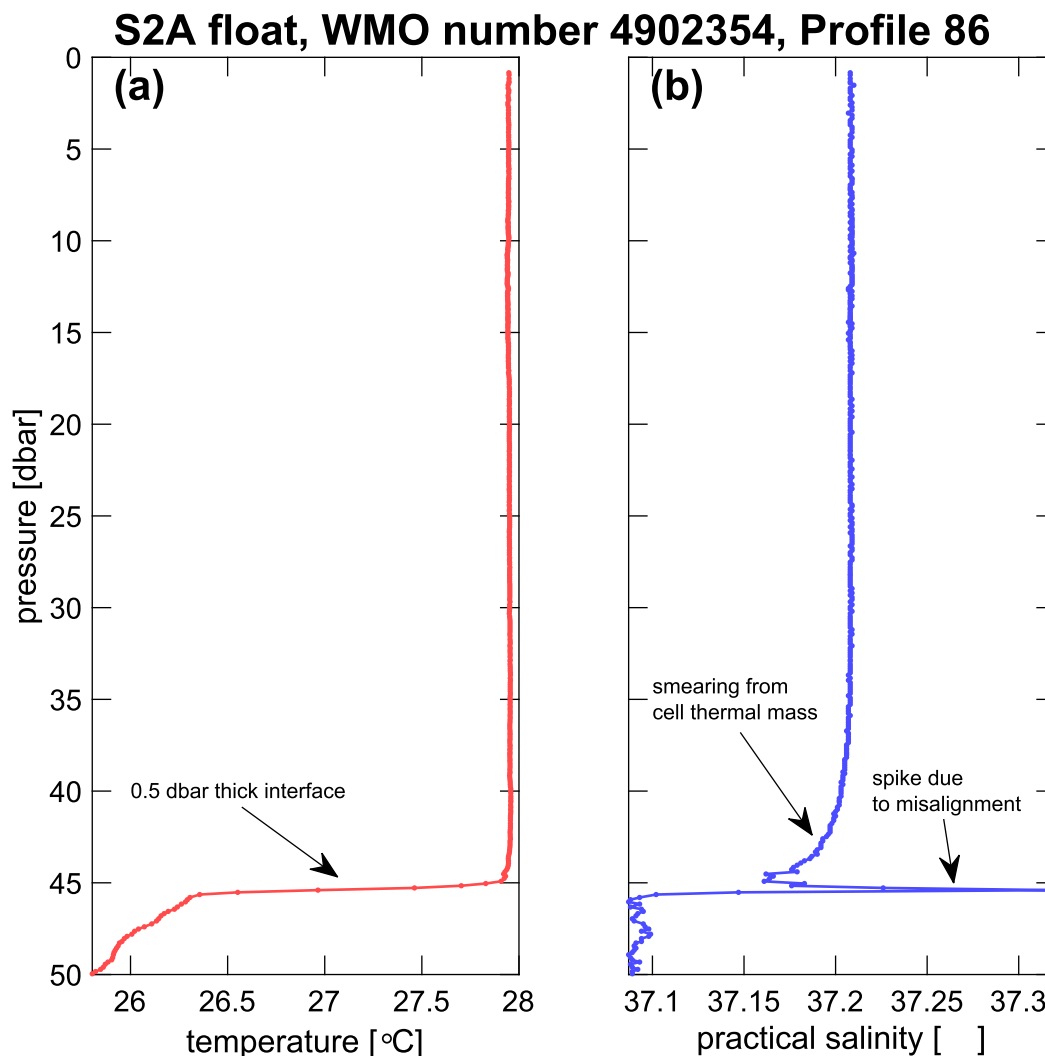


FIG. 1. Full-resolution 1 Hz (a) temperature and (b) salinity profile 86 from SOLO-II Argo float with WMO number 4902354 that reveals the effects of conductivity dynamic errors on salinity. The alignment error manifests as a spike at 45.5 m and the cell thermal mass error manifests as lag in salinity response, such that practical salinity is reduced above base of the mixed layer at 45.8 m.

However, these variables can be estimated a priori using conductivity. Conductivity is a function of both temperature and salinity. In the extreme artificial conditions of the stratified tank, the change in salinity accounts for more than 80% of the conductivity signal. This is in contrast to observations in the ocean, where temperature accounts for more than 80% of the conductivity signal. Therefore, the width and location of the salinity interface can be well described by the conductivity profile, which is done in [Martini et al. \(2019\)](#) and this paper.

The [Johnson \(2020\)](#) optimization is truncated before the conductivity cell reaches a steady state. Examination of the three profiles made in the stratified tank shows that at 5 times the cell thermal mass time scale (the final

salinity value as chosen by [Johnson 2020](#)) the conductivity is still increasing, while the temperature is not. This indicates that the temperature of the conductivity cell has not achieved equilibrium and calculated salinity still contains cell thermal mass error. The optimization will then result in a salinity profile that is always fresh of true. Furthermore, in all three profiles the conductivity in the bottom layer never completely stabilizes such that any optimization procedure that uses the profile data will always be biased fresh. We recognize that this is a limitation of the tank data, and therefore empirically pick the time of the maximum salinity and optimize until that salinity state is reached.

We argue that these three choices lead to results that are optimized to reduce the net variance against a poorly

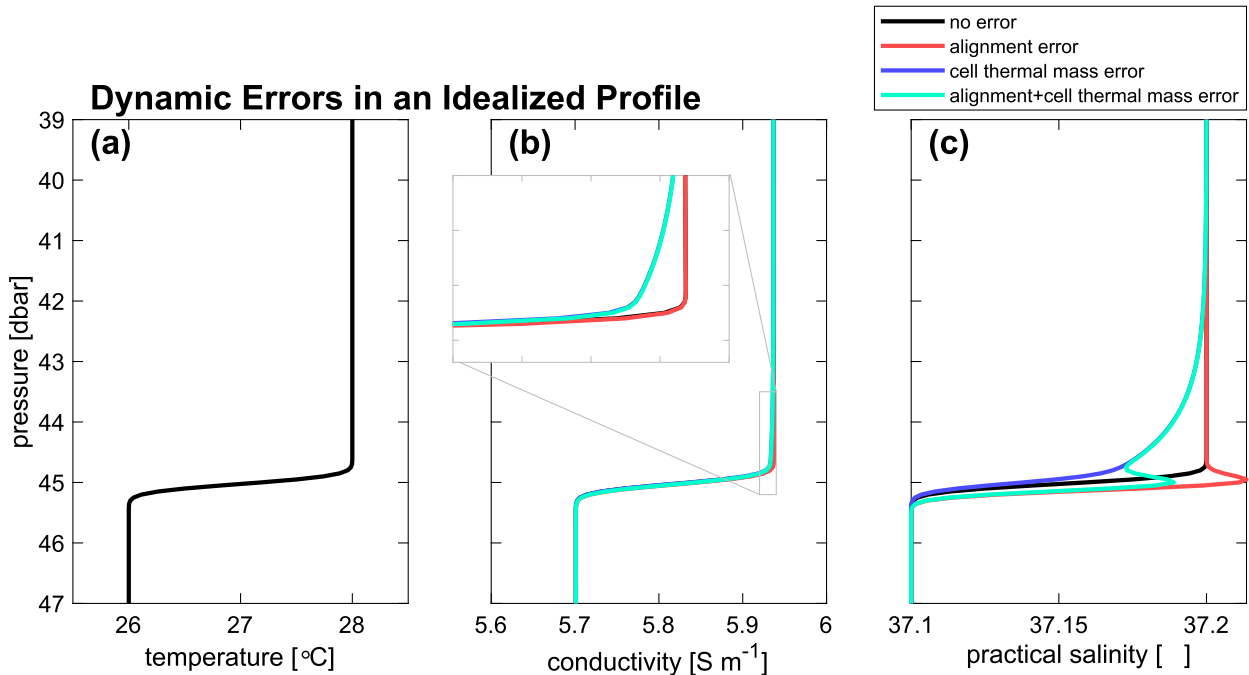


FIG. 2. Idealized error function model of the (a) high-resolution Argo temperature, (b) conductivity, and (c) practical salinity profiles presented in Fig. 1 with no dynamic error (black line), alignment error (red line), cell thermal mass error (blue line), and alignment plus cell thermal mass error (green line).

constrained statistical model that does not accurately represent physics (Figs. 1b,c in Johnson 2020). This ultimately results in more bias and error when applied to data outside of the stratified tank experiment as shown in section 5. However, pairing the error function (Johnson 2020) with physically realistic constraints on salinity (Martini et al. 2019) produces a more realistic model of the dominant physics in the tank and the conductivity cell. Optimizing against this model reduces the bias associated with both methods and produces improved corrections for in situ data.

3. Effect of alignment and cell thermal mass errors in situ

The effects of dynamic errors on Argo CTD data are most easily observed in the raw, full-resolution 1 Hz temperature, salinity and pressure data taken by the SBE 41CP. SOLO II floats deployed by the Scripps Institution of Oceanography regularly return data at this resolution from 0 to 50 m depth to study upper-ocean physics. These profiles capture the base of the mixed layer, which often features a large temperature and salinity gradient (Fig. 1). Like the stratified tank, large vertical gradients found in situ amplify dynamic errors. In the example here, the effect of the superposition of alignment and cell thermal mass errors and how they manifest as two

distinct features are shown. Alignment error, which is the temporal mismatch between temperature and conductivity error, produces a salinity spike within the interface

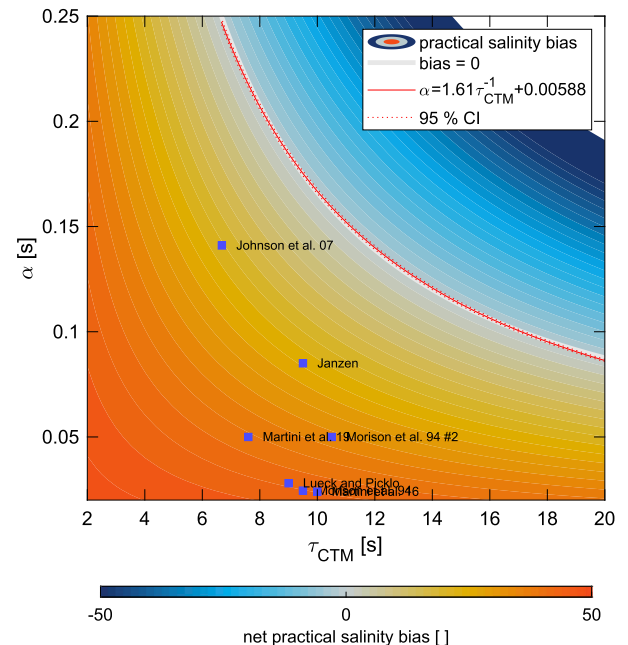


FIG. 3. Net practical salinity bias when the cell thermal mass correction coefficients, α and τ_{CTM} , are varied (color). Also shown are the zero bias contour (gray line), the fit to the zero bias contour (red line), and for comparison cell thermal mass correction coefficients from prior literature.

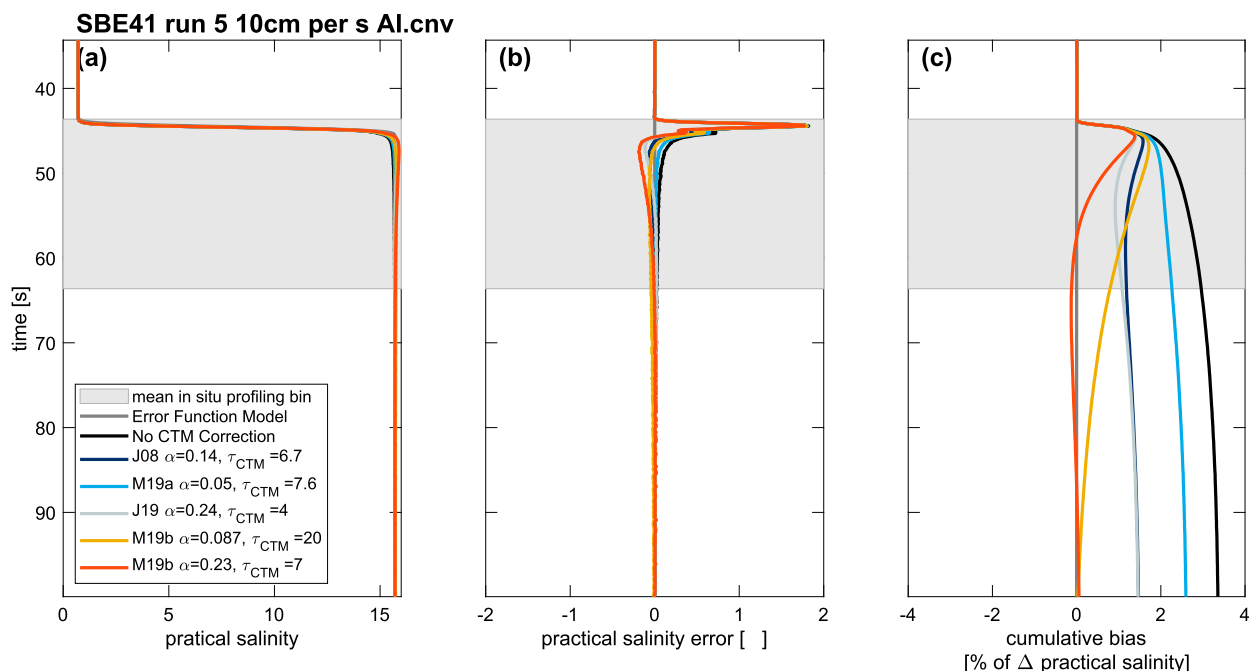


FIG. 4. Comparison of dynamic corrections to stratified tank data as determined in Johnson et al. (2007) (J08), Martini et al. (2019) (M19a), Johnson (2020) (J19), and this paper (M19b) against the uncorrected profile (black lines) and the idealized practical salinity (gray). Following Johnson (2020) the idealized practical salinity is an error function model. Shown are (a) the salinity profiles, (b) the practical salinity error, and (c) the cumulative practical salinity bias. The salinity error is the difference between each profile and the error function model. The cumulative bias is the cumulative sum of the error normalized by the net change in salinity over the gradient. If the cumulative bias does not return to zero, the correction is biased. Corrections from this paper are shown for cases of large τ_{CTM} and large α to illustrate their effect on the distribution of error within the profile, which must be considered when bin averaging. An example 2-m bin is denoted by the gray box in each panel.

at a depth of 45 dbar. Cell thermal mass error, which is an effect of the temperature difference between the seawater and the conductivity cell glass, creates a lagged response that manifests as decreased salinity nearly 10 dbar into the mixed layer.

The salinity spike and smearing shown in Fig. 1 can be reproduced by adding alignment and cell thermal mass error to an idealized model of the in situ temperature and salinity profile (black lines, Fig. 2). Used here are an alignment correction determined from in situ profiles of this float (0.6 s) and 1 Hz cell thermal mass correction coefficients as determined in Martini et al. (2019) for a float profiling at 0.05 m s^{-1} . In this case, where temperature and salinity decrease with depth, practical salinity is positively biased when alignment is the only source of error (1.007) and negatively biased when cell thermal mass is the only source of error (-0.652). The net bias from the superposition of alignment and cell thermal mass errors is positive (0.355). In this example, the alignment error is larger than cell thermal mass error leading to a net positive bias, but this may not be the case where the temperature and salinity structure differs.

4. Cell thermal mass corrections

The error function method presented by Johnson (2020) is used to determine the correction coefficients for cell thermal mass.¹ This method produces a set of solutions where $\alpha \times \tau_{CTM}$ equals a constant (Fig. 3). For profiling speeds of 0.05, 0.10, and 0.15 m s^{-1} , $\alpha \times \tau_{CTM} = 1.64, 1.61, \text{ and } 1.49$, respectively. The consistency between these values indicate the error function method is robust; however, a second set of conditions is needed to determine the optimal α and τ_{CTM} pair.

Although the set of solutions minimizes the net bias over the gradient, choosing the incorrect set of α and τ_{CTM} can still lead to bias when the profile data are bin averaged (Fig. 4). Choosing an α that is too large results in spikes isolated to a single bin. Choosing a τ_{CTM} that is too large results in bias smeared across multiple bins.

¹The conductivity data have already been corrected for alignment using the 16 Hz coefficients determined in Martini et al. (2019). The idealized model of practical salinity in the stratified tank is an error function defined by the practical salinity range and the interface thickness determined in Martini et al. (2019).

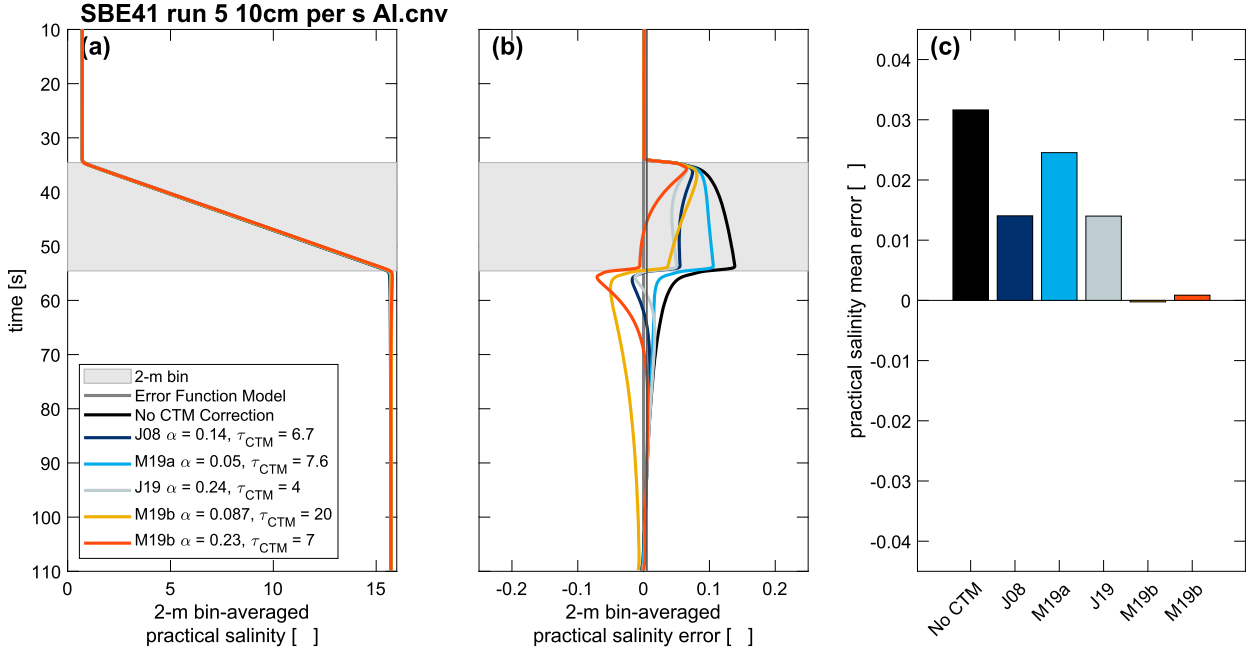


FIG. 5. Comparison of dynamic corrections to binned stratified tank data as determined in Johnson et al. (2007) (J08), Martini et al. (2019) (M19a), Johnson (2020) (J19), and this paper (M19b) against the binned uncorrected profile (black lines) and the binned idealized practical salinity (gray). Shown are (a) the binned profiles, (b) the binned practical salinity error, and (c) the mean practical salinity error (or total bias) for each correction.

Thus, there are multiple metrics that can be used to determine the optimal coefficients. In the spirit of the prior analysis in Martini et al. (2019), we find the α and τ_{CTM} pair that minimizes the overall bias in binned data. Other choices could be a pair that constrains error to a single bin or reduces the magnitude of the largest salinity spike.

Binned profiles equivalent to those telemetered from Argo floats are generated by running a 2-m boxcar filter over the uncorrected and corrected salinity profiles in order to produce all possible permutations of the binning algorithm (Fig. 5a). Because the numerical correction is only a first-order approximation of the cell thermal mass effect and the optimized coefficients are determined by reducing the net bias over the entire profile, there is no combination of α and τ_{CTM} that will result in zero error for every bin (Fig. 5b). Nonetheless, minimizing the average practical salinity error in the binned profiles can serve as the second condition needed to determine the cell thermal mass

correction coefficients to minimize bias in binned Argo data. The optimized coefficient pairs are listed in Table 1. Even if not optimized with the second condition, the example cell thermal mass correction coefficients used in Fig. 5 produce profiles with less bias than Johnson et al. (2007), Martini et al. (2019), and Johnson (2020).

Following the same methods used in Martini et al. (2019), the 16 Hz corrections are adapted for sampling at 1 Hz. The results are presented in Table 2.

5. Efficacy of the corrections on in situ data

The efficacy of applying the different correction coefficients determined in Johnson et al. (2007), Martini et al. (2019), Johnson (2020), and this paper are shown in Fig. 6. The same profile is used as in Fig. 1, and it is expected that the practical salinity profile will be a step change like the temperature profile. The profiles corrected using the Martini et al. (2019), and this paper)

TABLE 1. Correction coefficients for pumped SBE 41CP sampling at 16 Hz determined from the stratified tank experiment.

Profile No.	Profiling speed (m s^{-1})	f_s (Hz)	τ_T (s)	t_p (s)	α	τ_{CTM} (s)
3	0.05	16	0.47	0	0.129	12.5
5	0.10	16	0.47	0.1250	0.152	11
6	0.15	16	0.50	0.1250	0.132	12.5

TABLE 2. Correction coefficients for pumped SBE 41CP sampling at 1 Hz determined from subsampling 16 Hz data from the stratified tank experiment.

Profile No.	Profiling speed (m s^{-1})	f_s (Hz)	τ_T (s)	t_P (s)	α	τ_{CTM} (s)
3	0.05	1	0.21	-0.19	0.035	11.8
5	0.10	1	0.16	-0.26	0.090	9.16
6	0.15	1	0.23	-0.25	0.110	12.2

coefficients most closely approximate this idealized model, while the [Johnson et al. \(2007\)](#) and [Johnson \(2020\)](#) corrected profiles amplify the practical salinity spike within the interface. The spiking is caused by insufficient corrections for alignment and large values of α .

6. Conclusions

The stratified tank analysis is vital to understanding dynamic errors in the SBE 41CP. The analysis presented in [Martini et al. \(2019\)](#) revealed the contributions of alignment and cell thermal mass to salinity spiking, which could then be verified with data from Argo floats ([Figs. 1 and 6](#)). The corrections from [Martini et al. \(2019\)](#), and this paper) appear to be closer to correct, but it is only a single profile and what is truly correct is only an assumption.

We therefore cannot recommend that any of the corrections in [Johnson et al. \(2007\)](#), [Martini et al. \(2019\)](#), [Johnson \(2020\)](#), and this paper be applied to binned or unbinned Argo data. A more vigorous statistical approach using in situ data is needed. This can be done with the full-resolution, unbinned, 1-Hz CTD data from SBE 41CP deployed on SOLO II Argo floats. By using in situ Argo float data, we remove ambiguity associated with the following:

- Interpolating 16 Hz data to determine corrections for 1 Hz sampling.
- Variations in cell thermal mass response due to differences in profiling speeds on the different platforms ([Martini et al. 2019](#); [Johnson et al. 2007](#)). Mean profiling speed for Argo floats and ITPs are 0.1 and 0.27 m s^{-1} , respectively.

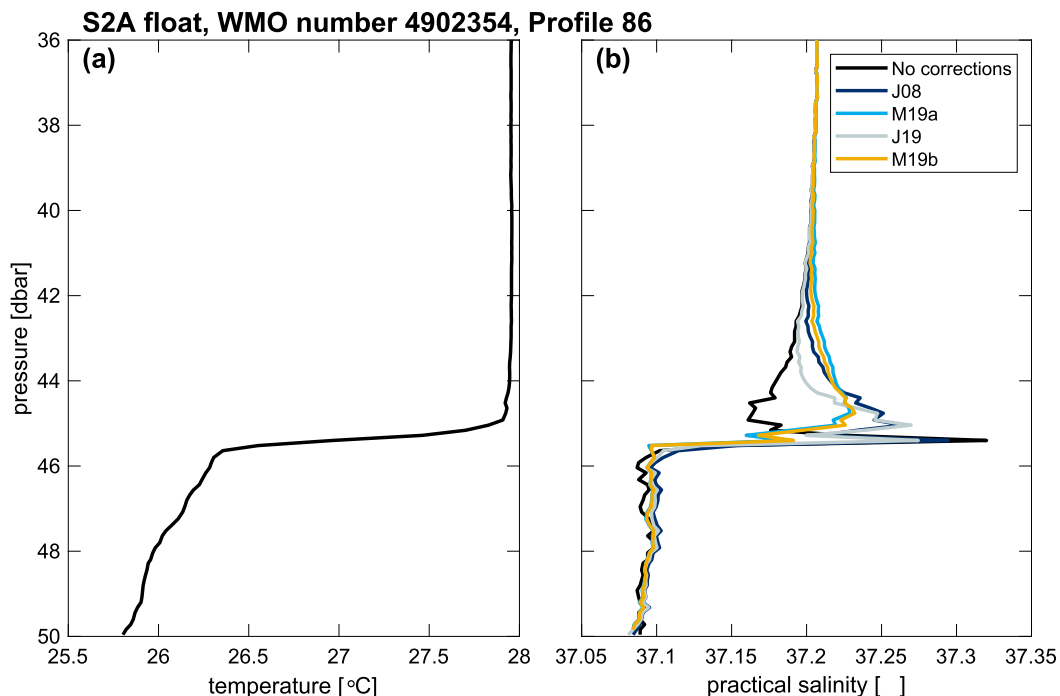


FIG. 6. Comparison of dynamic corrections to practical salinity using in situ data from SOLO-II Argo float with WMO number 4902354. Plotted are (a) temperature and (b) practical salinity profiles with alignment and cell thermal mass corrections from [Johnson et al. \(2007\)](#) (J08), [Martini et al. \(2019\)](#) (M19a), [Johnson \(2020\)](#) (J19), and this paper (M19b) applied. The [Johnson \(2020\)](#) correction is consistent with the methods in the paper, where the cell thermal mass correction is applied before aligning temperature and conductivity.

- Changes in SBE 41CP CTD sampling associated with firmware revisions.

These optimized corrections are the topic of a forthcoming paper and will provide robust recommendations for handling data from the entire fleet of SBE 41CPs deployed on Argo floats.

Acknowledgments. Thanks to Pelle Robbins for finding the in situ profiles used for this analysis in the vast database of Argo floats, John Gilson showing me how to access that high-resolution data, Ray Schmitt for use of the stratified tank, Susan Wijffels, Breck Owens, and Annie Wong for intellectual support, and Diego Sorrentino and Vlad Simontov for validating the sampling scheme in the SBE 41CP.

REFERENCES

- Johnson, G. C., 2020: Comment on “Corrections for pumped SBE 41CP CTDs determined from stratified tank experiments.” *J. Atmos. Oceanic Technol.*, **37**, 351–355, <https://doi.org/10.1175/JTECH-D-19-0098.1>.
- , J. M. Toole, and N. G. Larson, 2007: Sensor corrections for Sea-Bird SBE-41CP and SBE-41 CTDs. *J. Atmos. Oceanic Technol.*, **24**, 1117–1130, <https://doi.org/10.1175/JTECH2016.1>.
- Martini, K. I., D. J. Murphy, R. W. Schmitt, and N. G. Larson, 2019: Corrections for pumped SBE 41CP CTDs determined from stratified tank experiments. *J. Atmos. Oceanic Technol.*, **36**, 733–744, <https://doi.org/10.1175/JTECH-D-18-0050.1>.
- Schmitt, R. W., R. C. Millard, J. M. Toole, and W. D. Wellwood, 2005: A double-diffusive interface tank for dynamic-response studies. *J. Mar. Res.*, **63**, 263–289, <https://doi.org/10.1357/0022240053693842>.